SUPPLEMENTARY MATERIAL

How to measure the ESR intensity of the Al centre in optically bleached coarse quartz grains for dating purpose?

Ben Arous, Eslem[a,b,c], Duttine, Mathieu[4], Duval, Mathieu[a,e,f]

[a]Centro Nacional de Investigación sobre la Evolución Humana (CENIEH), Burgos, Spain

[b]Max Planck Institute for Geoanthropology, Pan-African Evolution Research Group, Jena, Germany

[c]Museum national d'Histoire naturelle, Histoire naturelle de l'Homme préhistorique, Paris, France

[4]Institut de Chimie de la Matière Condensée de Bordeaux (ICMCB), Univ. Bordeaux, CNRS, Bordeaux INP, Pessac, France

[e]Australian Research Centre for Human Evolution (ARCHE), Griffith University, Brisbane, Australia

[f] Palaeoscience Labs, Dept. Archaeology and History, La Trobe University, Melbourne Campus, Bundoora, Victoria, Australia

*corresponding author: ben-arous@gea.mpg.de

Figure S1. ESR DRCs based on the Al signal measured in sample #1, whose intensity has been obtained from the four methods presented in this paper.

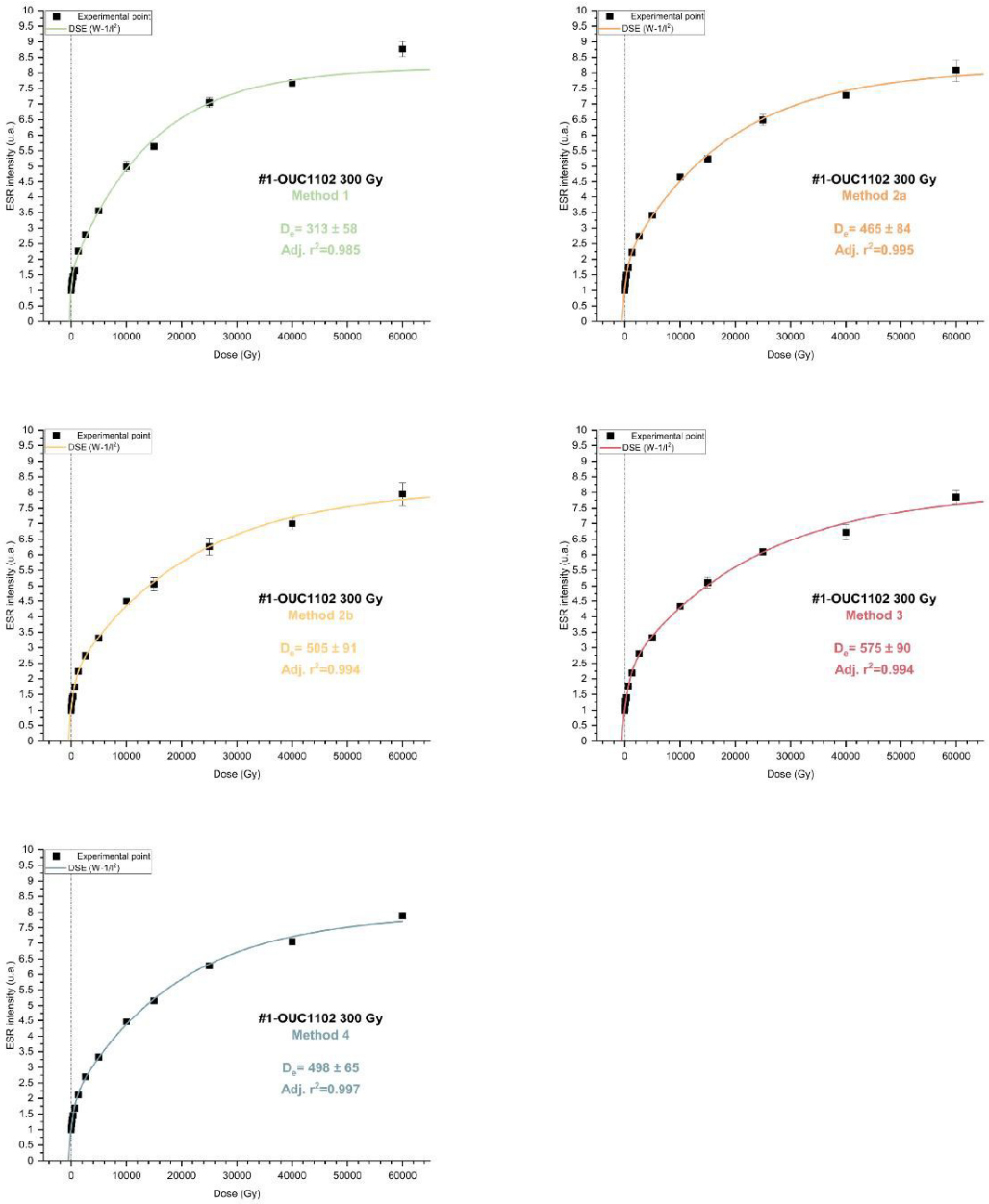

Figure S2. ESR DRCs based on the Al signal measured in sample #2, whose intensity has been obtained from the four methods presented in this paper.

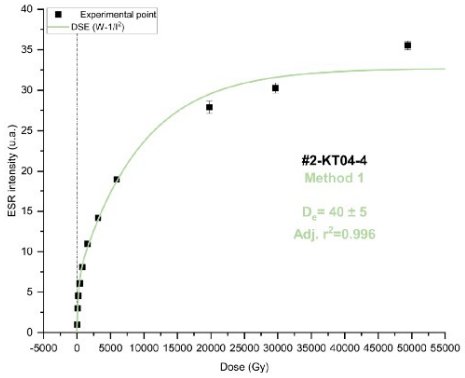

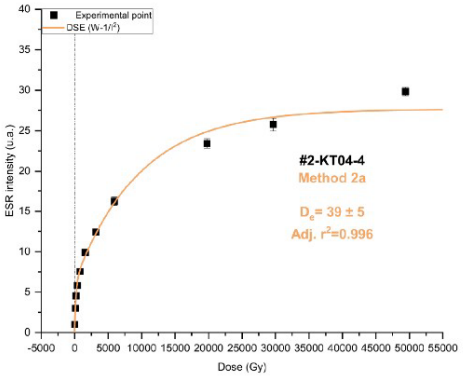

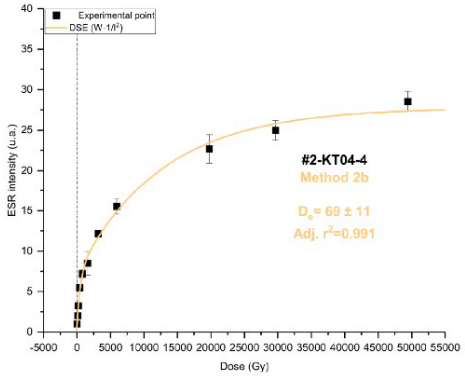

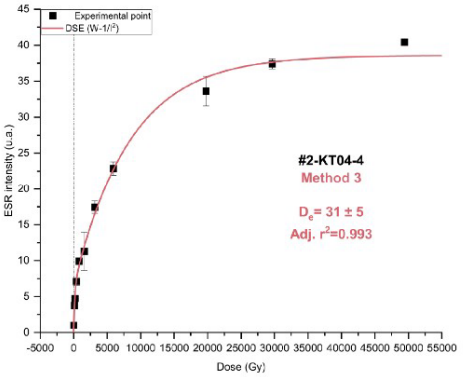

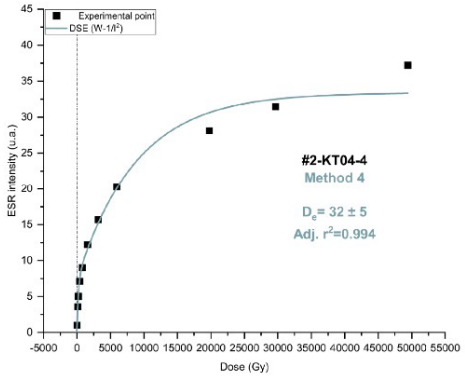

Figure S3. ESR DRCs based on the Al signal measured in sample #3, whose intensity has been obtained from the four methods presented in this paper.

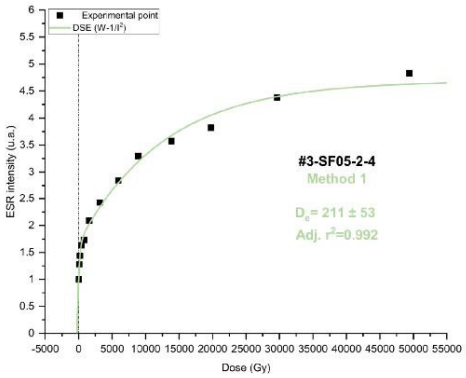

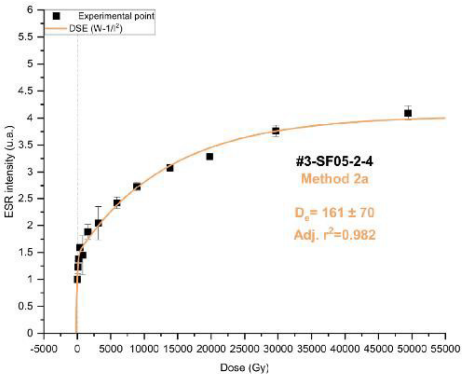

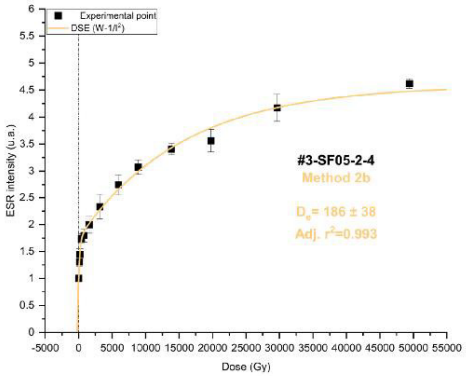

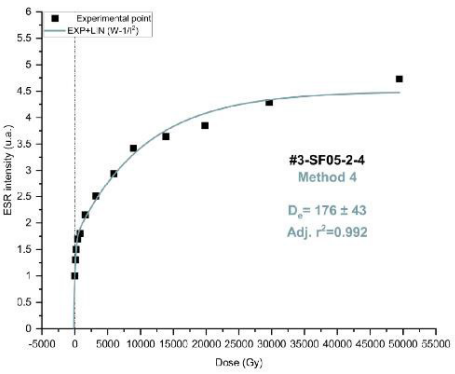

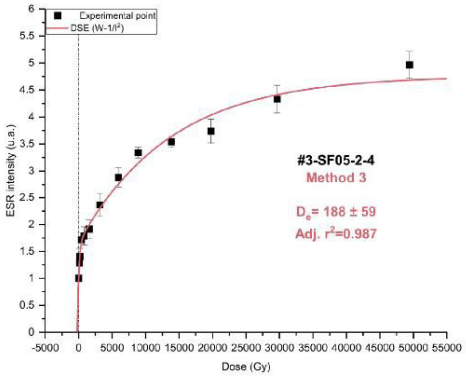

Figure S4. ESR DRCs based on the Al signal measured in sample #4, whose intensity has been obtained from the four methods presented in this paper.

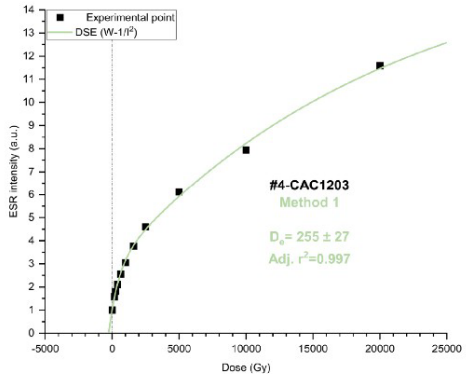

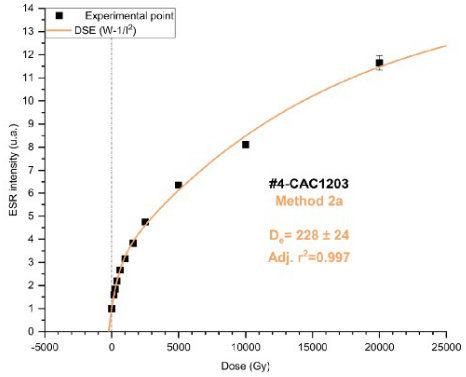

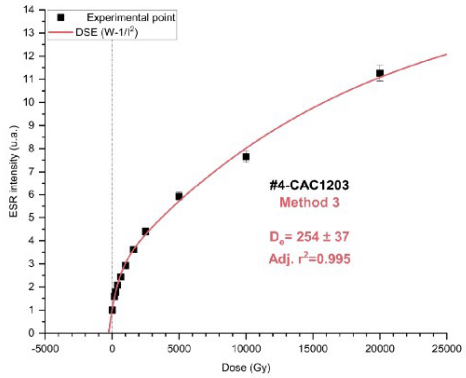

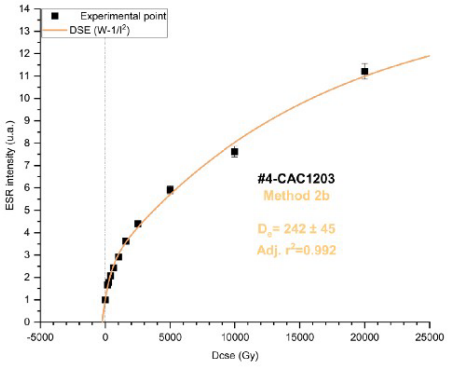

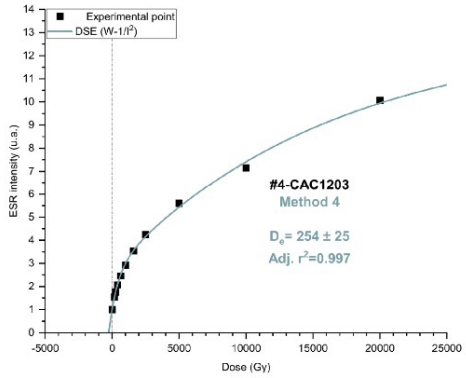

Figure S5. ESR DRCs based on the Al signal measured in sample #5, whose intensity has been obtained from the four methods presented in this paper.

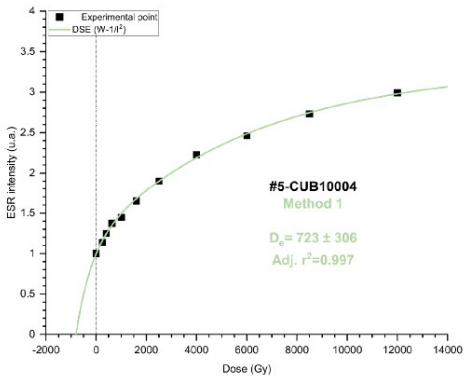

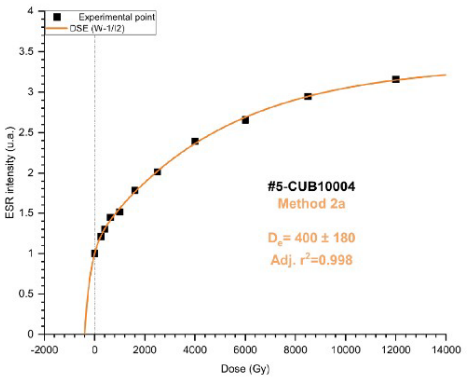

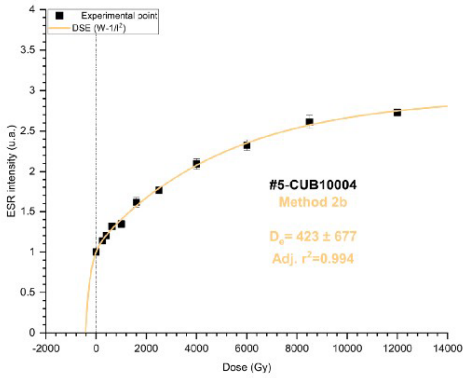

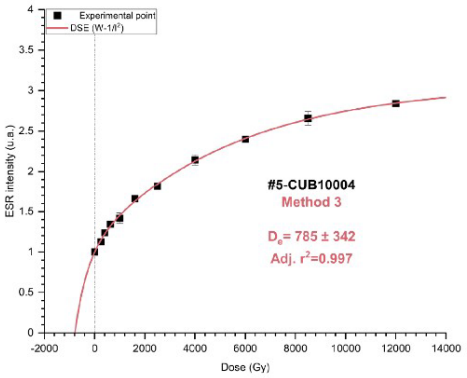

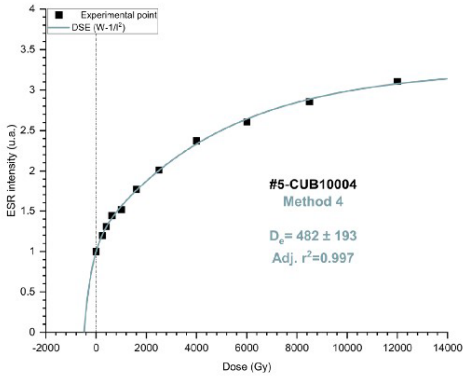

Figure S7. ESR DRCs based on the Al signal measured in sample #6, whose intensity has been obtained from the four methods presented in this paper.

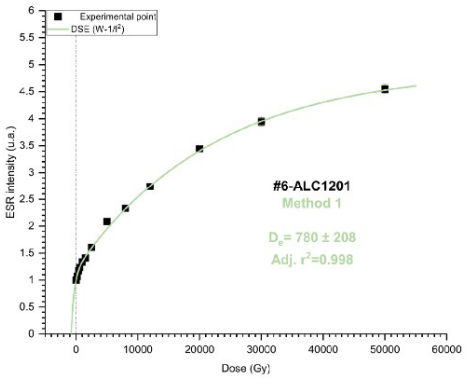

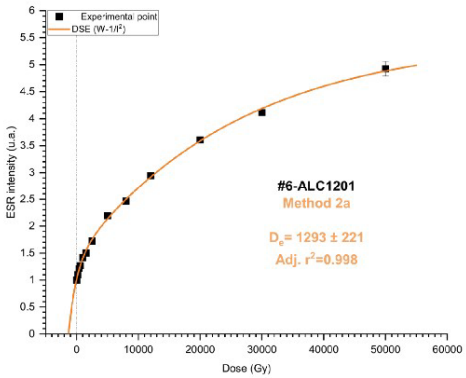

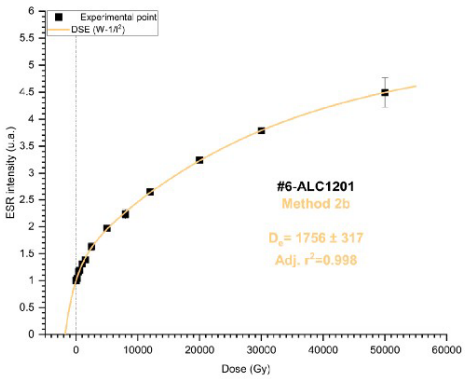

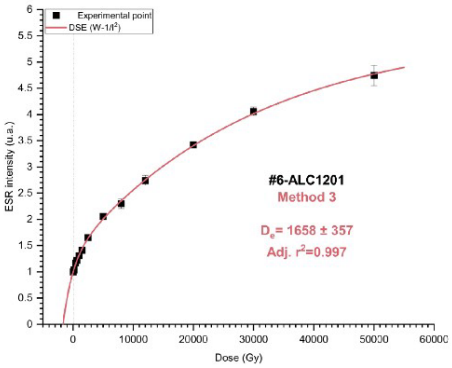

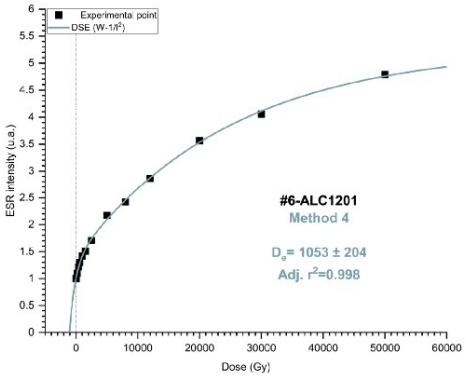

Figure S8. ESR DRCs based on the Al signal measured in sample #7, whose intensity has been obtained from the four methods presented in this paper.

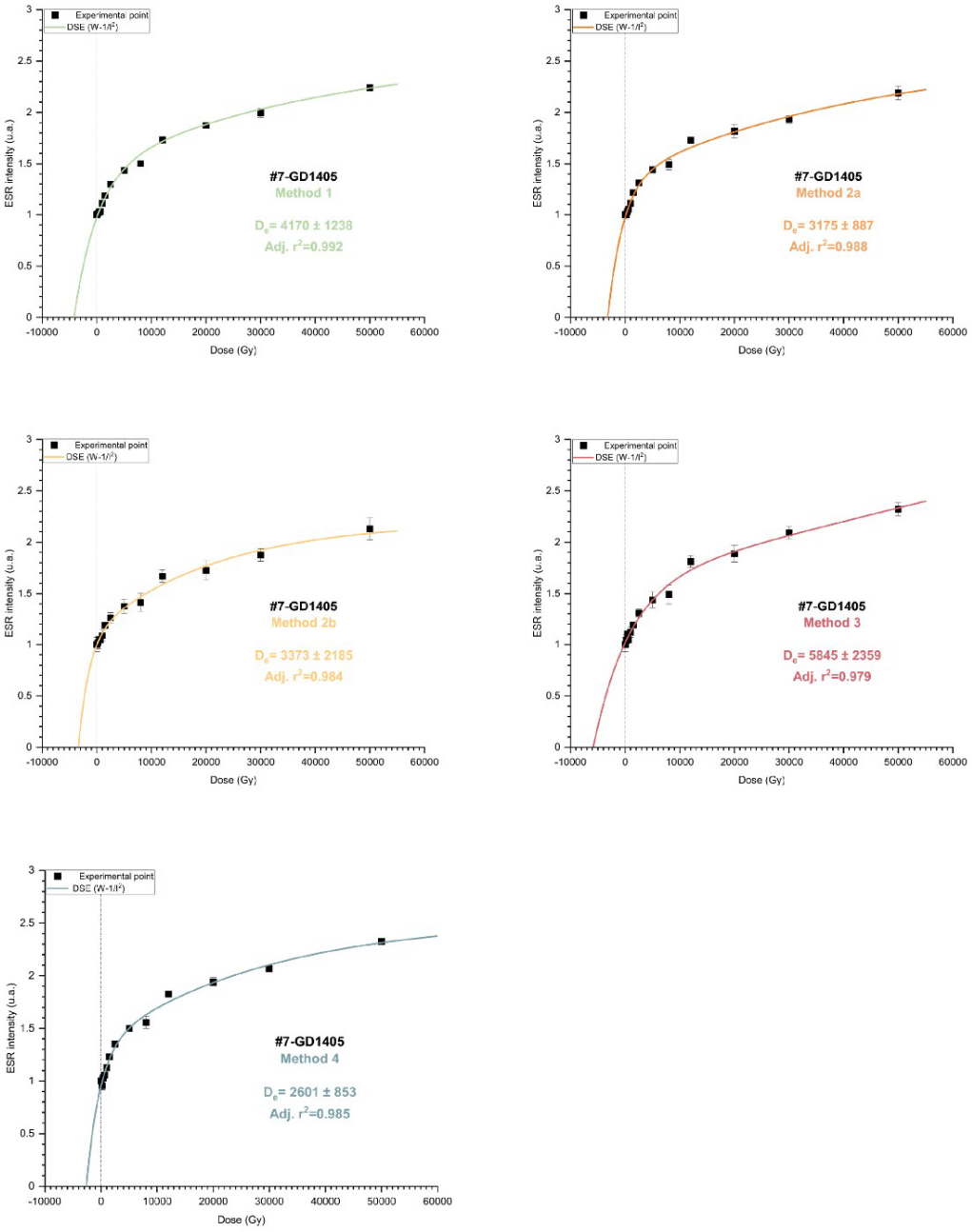

Figure S8. ESR DRCs based on the Al signal measured in sample #8, whose intensity has been obtained from the four methods presented in this paper.

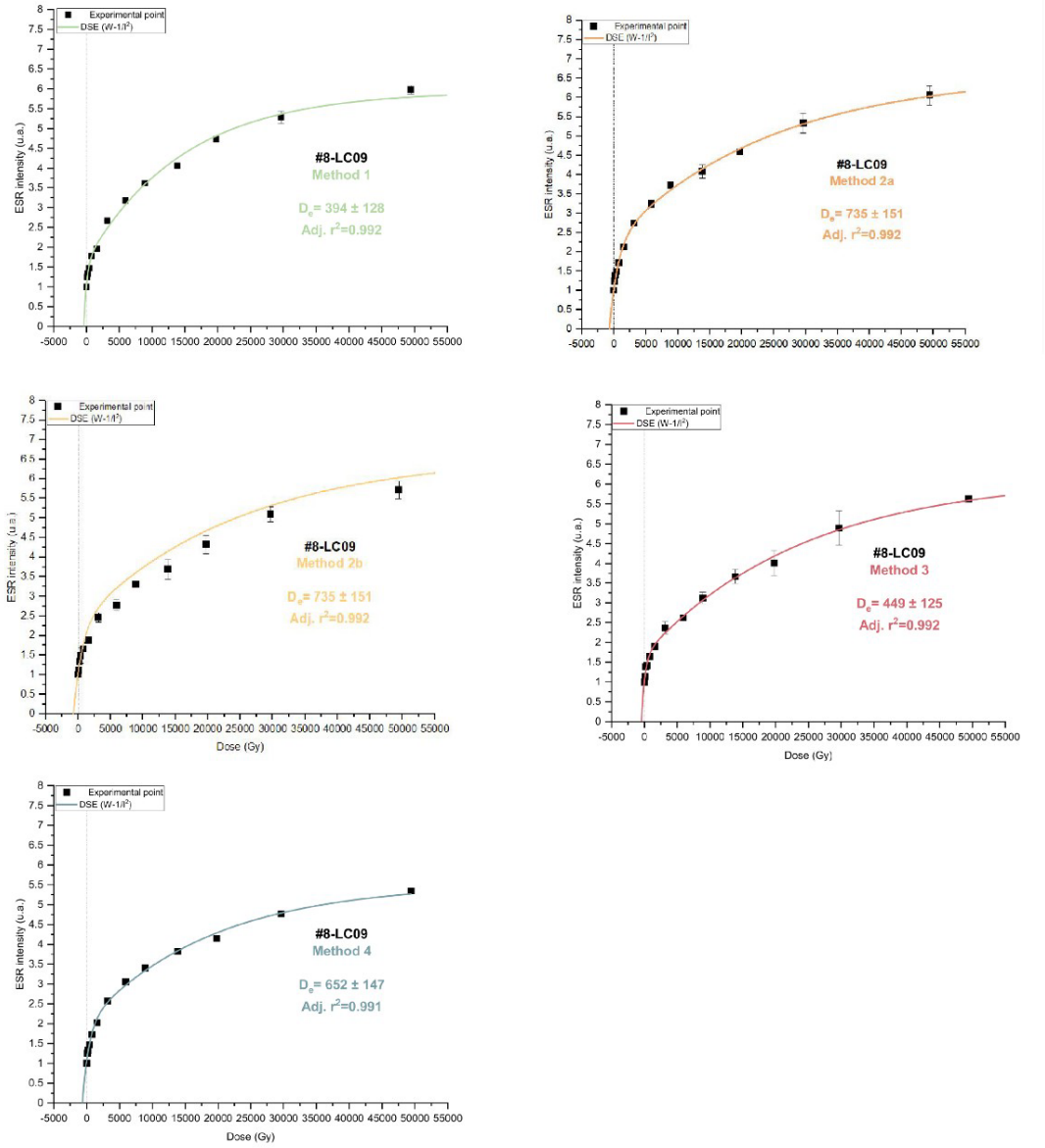

Figure S9. Comparison of Al signal measured in various aliquots of the eight quartz samples.

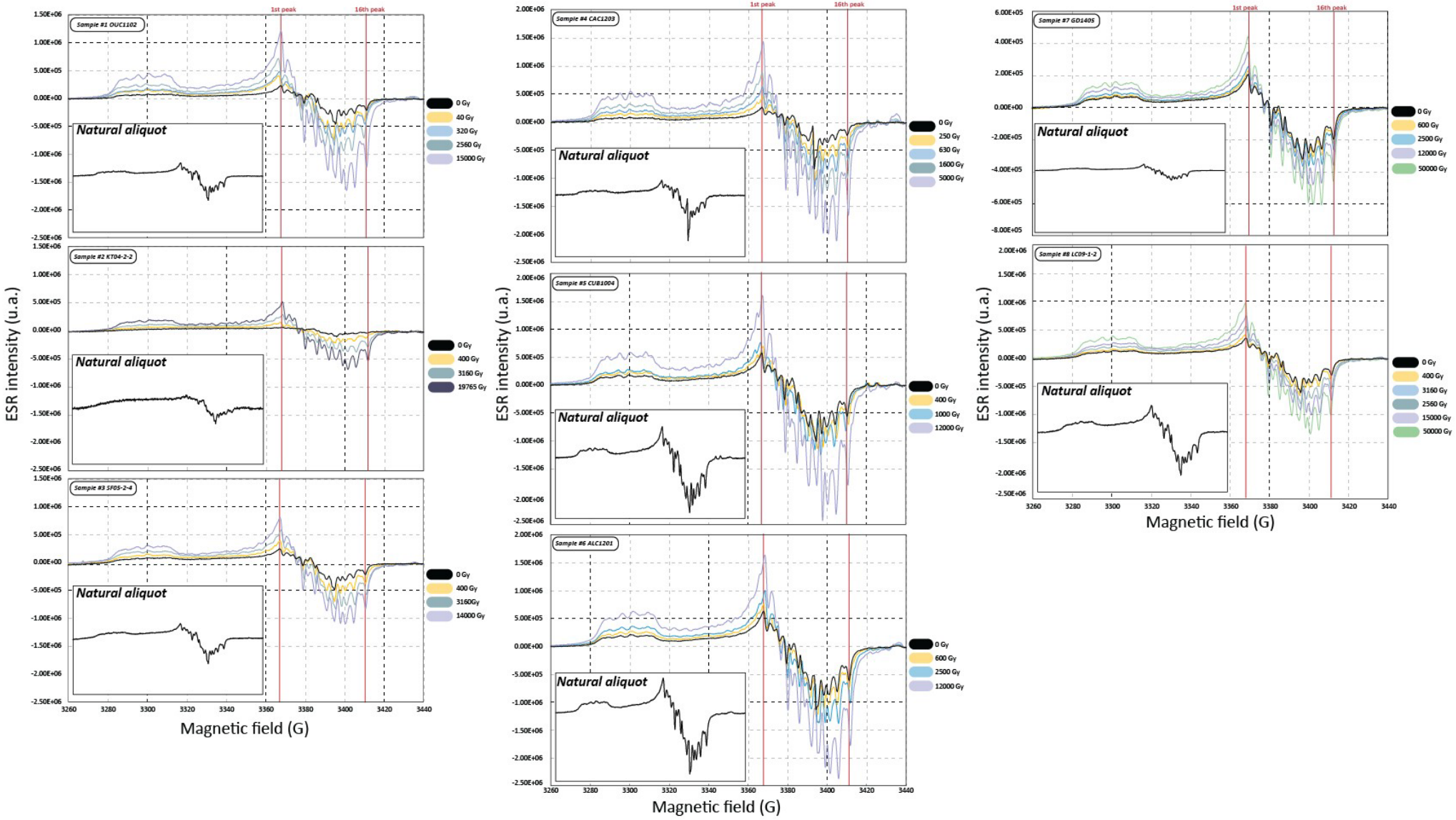

Figure S10. Comparison of the number of peaks per sample. Only the natural aliquot spectrum of each quartz sample is represented. All spectra were aligned with respect to the first peak. For sample #2, the signal intensity has been multiplied by a factor 6 and by 4 for the sample #4.

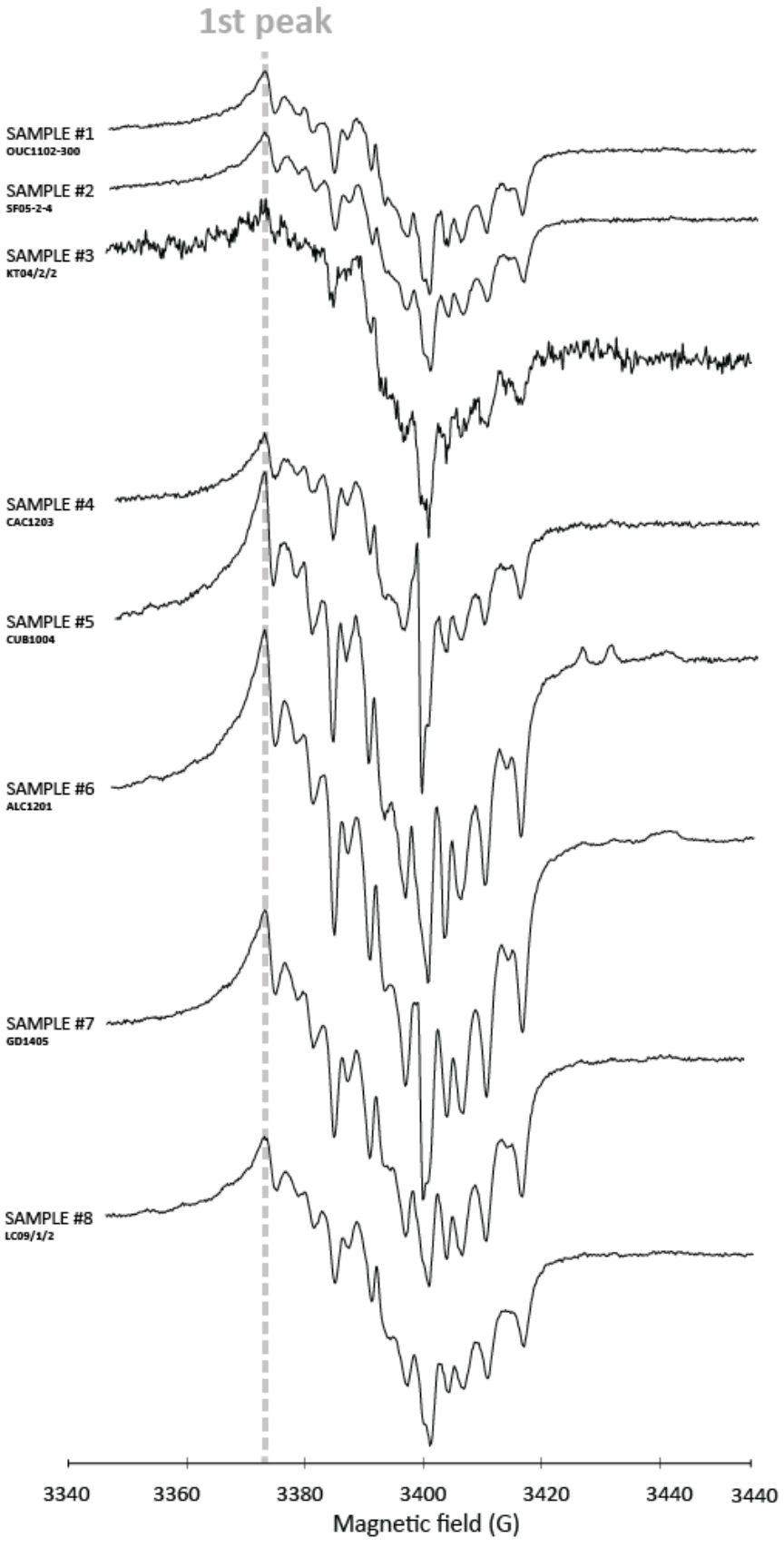

Figure S13. Comparison of the natural spectra of the sample #1 at low temperature (A), at room temperature with 2 mW and 10 mW (B). A basic visualization of the signal at room temperature is given in C.

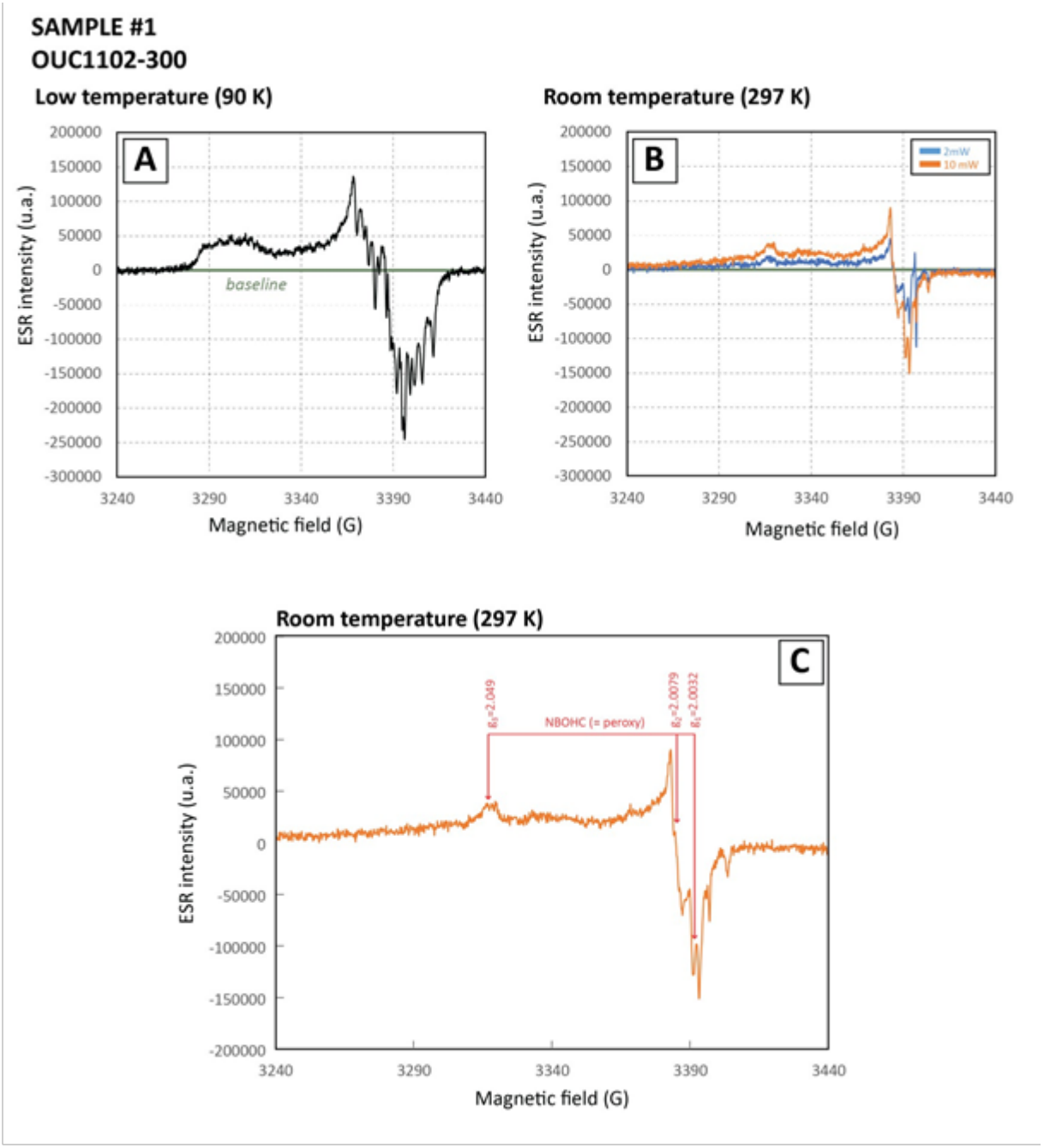

Figure S14. Comparison of the natural spectra of the sample #2 at low temperature (A), at room temperature with 2mW and 10 mW (B). A basic visualization of the signal at room temperature is given in C.

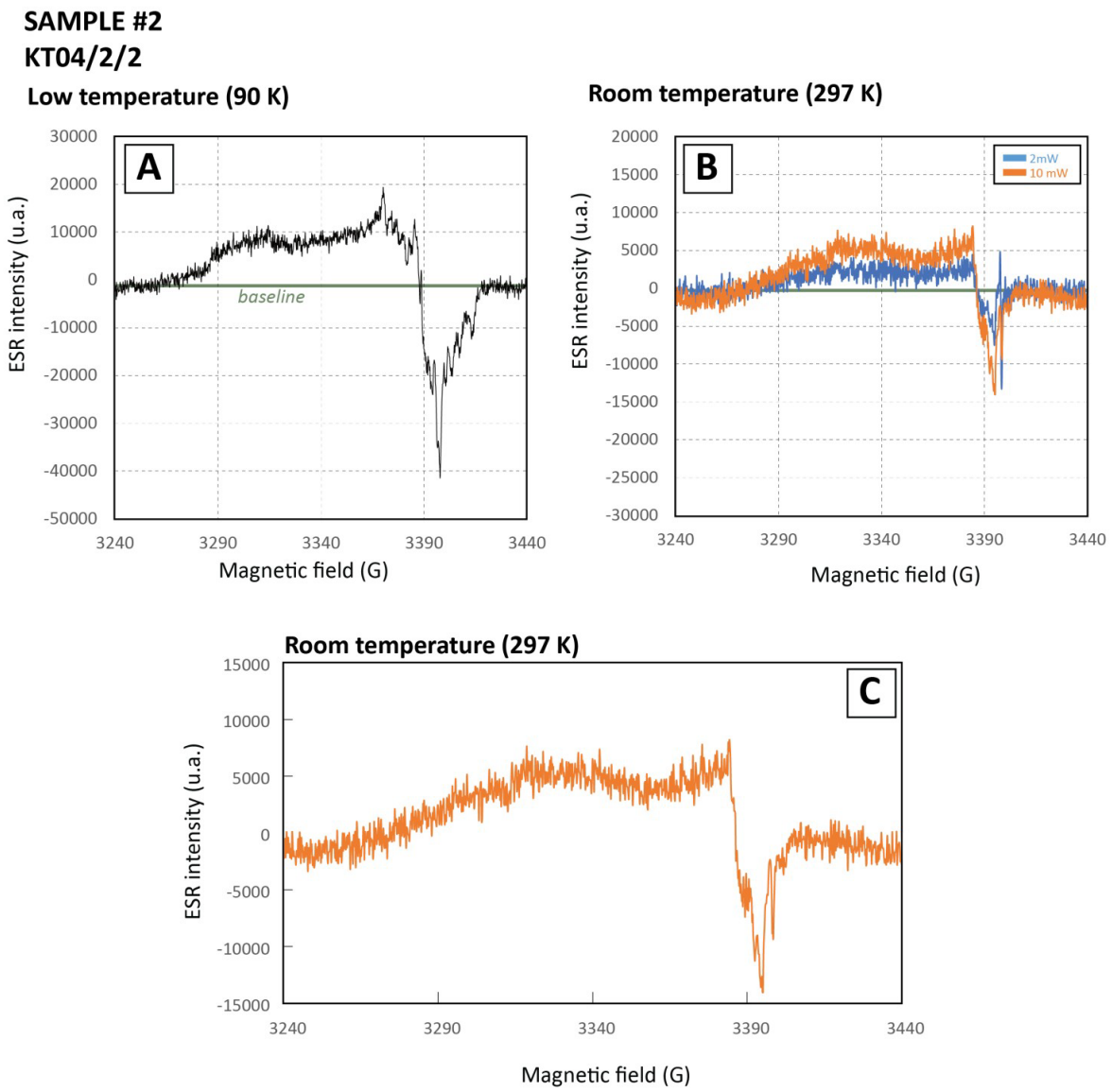

Figure S13. Comparison of the natural spectra of the sample #3 at low temperature (A), at room temperature with 2mW and 10 mW (B). A basic visualization of the signal at room temperature is given in C.

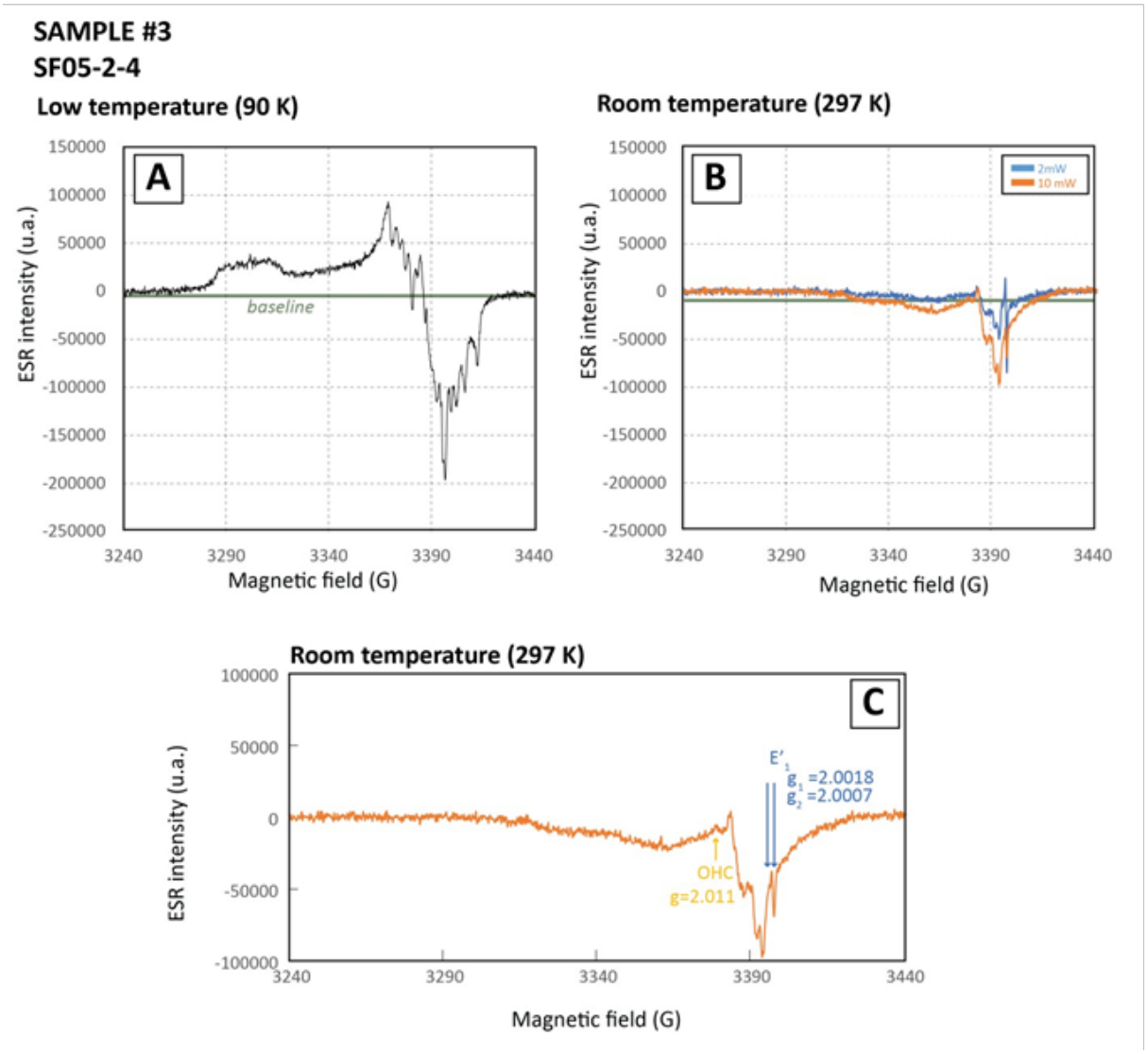

Figure S14. Comparison of the natural spectra of the sample #4 at low temperature (A), at room temperature with 2 mW and 10 mW (B). A basic visualization of the signal at room temperature is given in C. For the identification of SO_3 centre, see in detail Ikeda et al. (1992) and Ryabov et al. (1983).

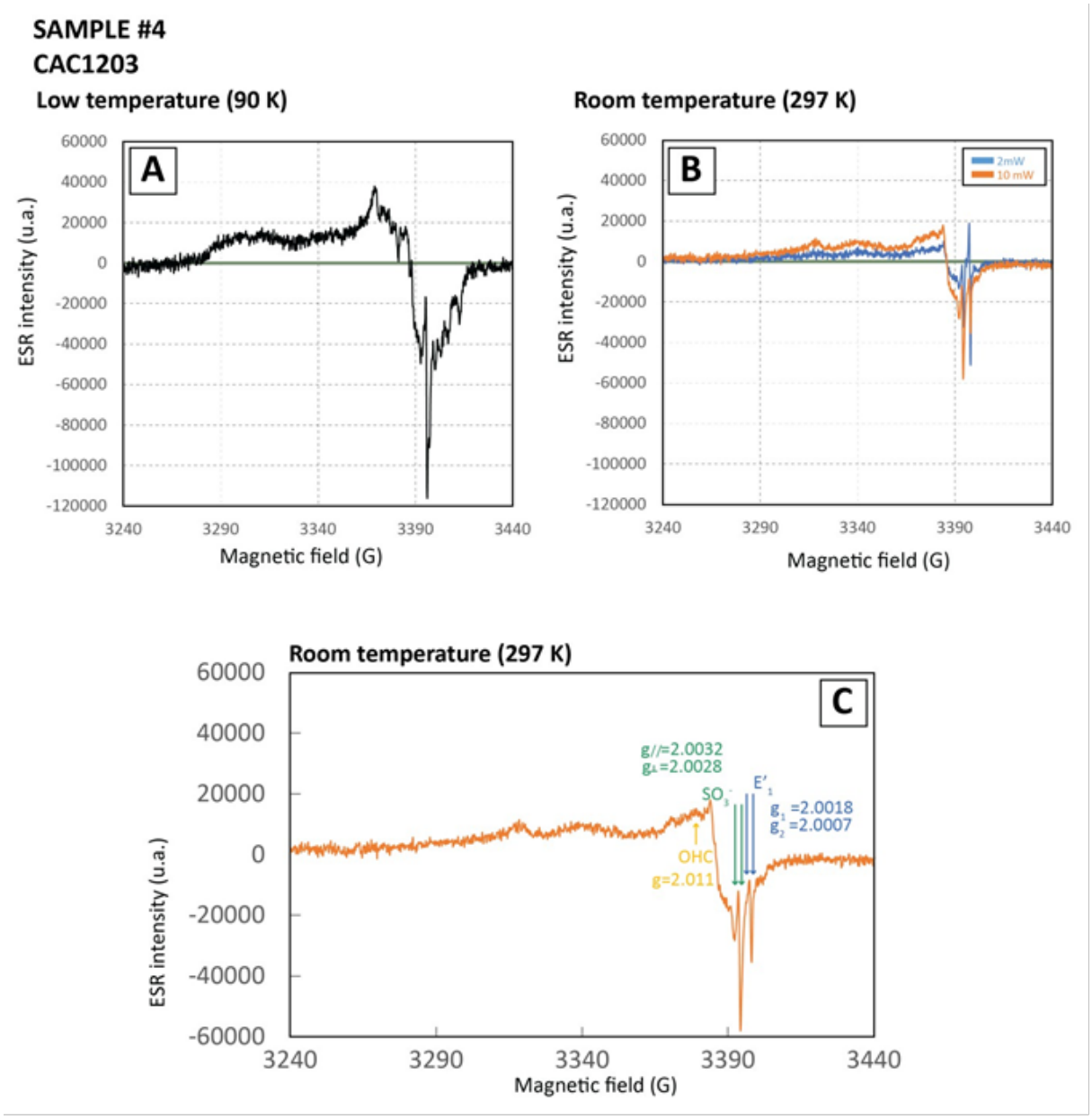

Figure S15. Comparison of the natural spectra of the sample #5 at low temperature (A), at room temperature with 2 mW and 10 mW (B). A basic visualization of the signal at room temperature is given in C.

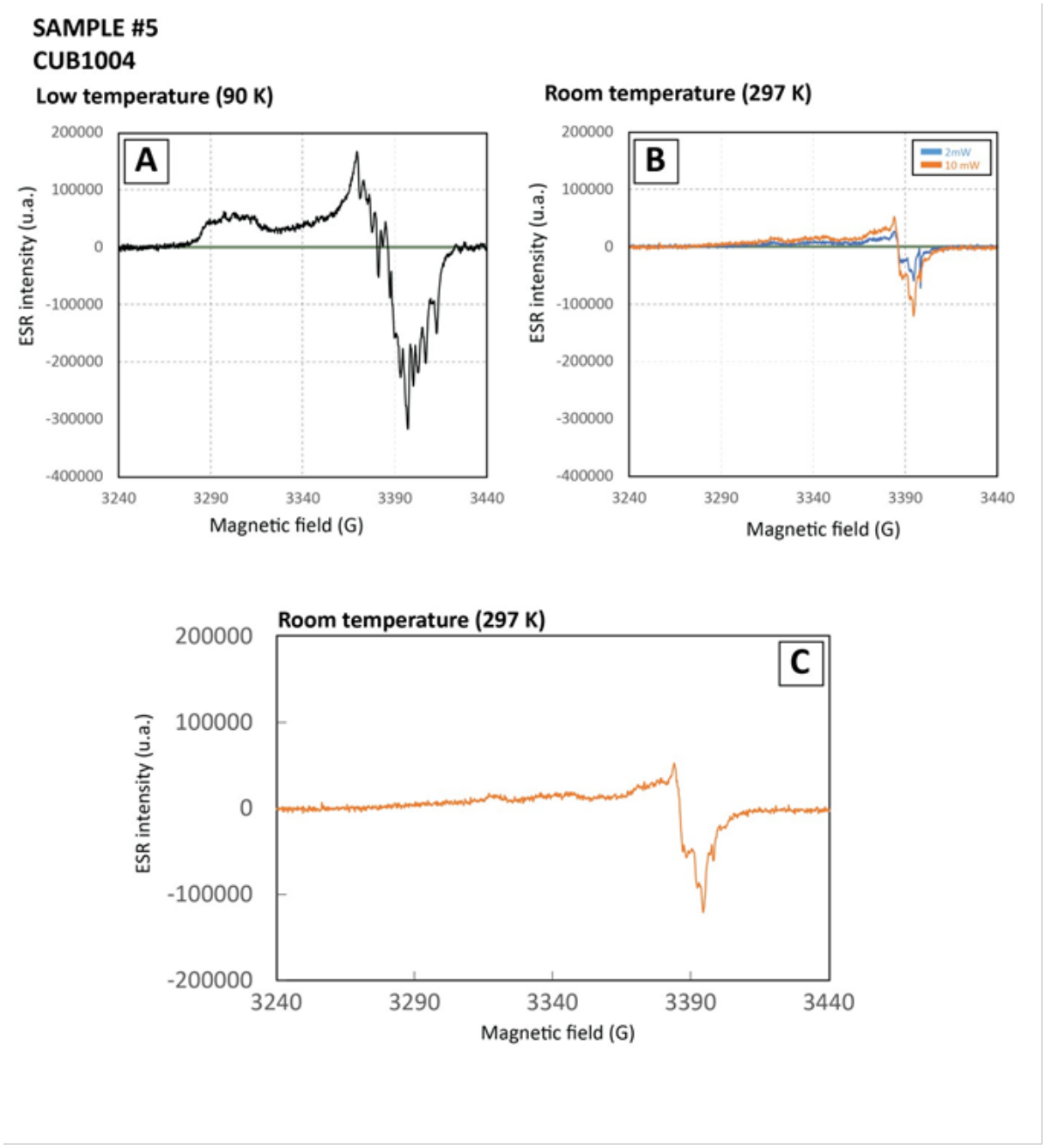

Figure S16. Comparison of the natural spectra of the sample #6 at low temperature (A), at room temperature with 2mW and 10 mW (B). A basic visualization of the signal at room temperature is given in C. For the identification of SO_3 centre, see in detail Ikeda et al. (1992) and Ryabov et al. (1983).

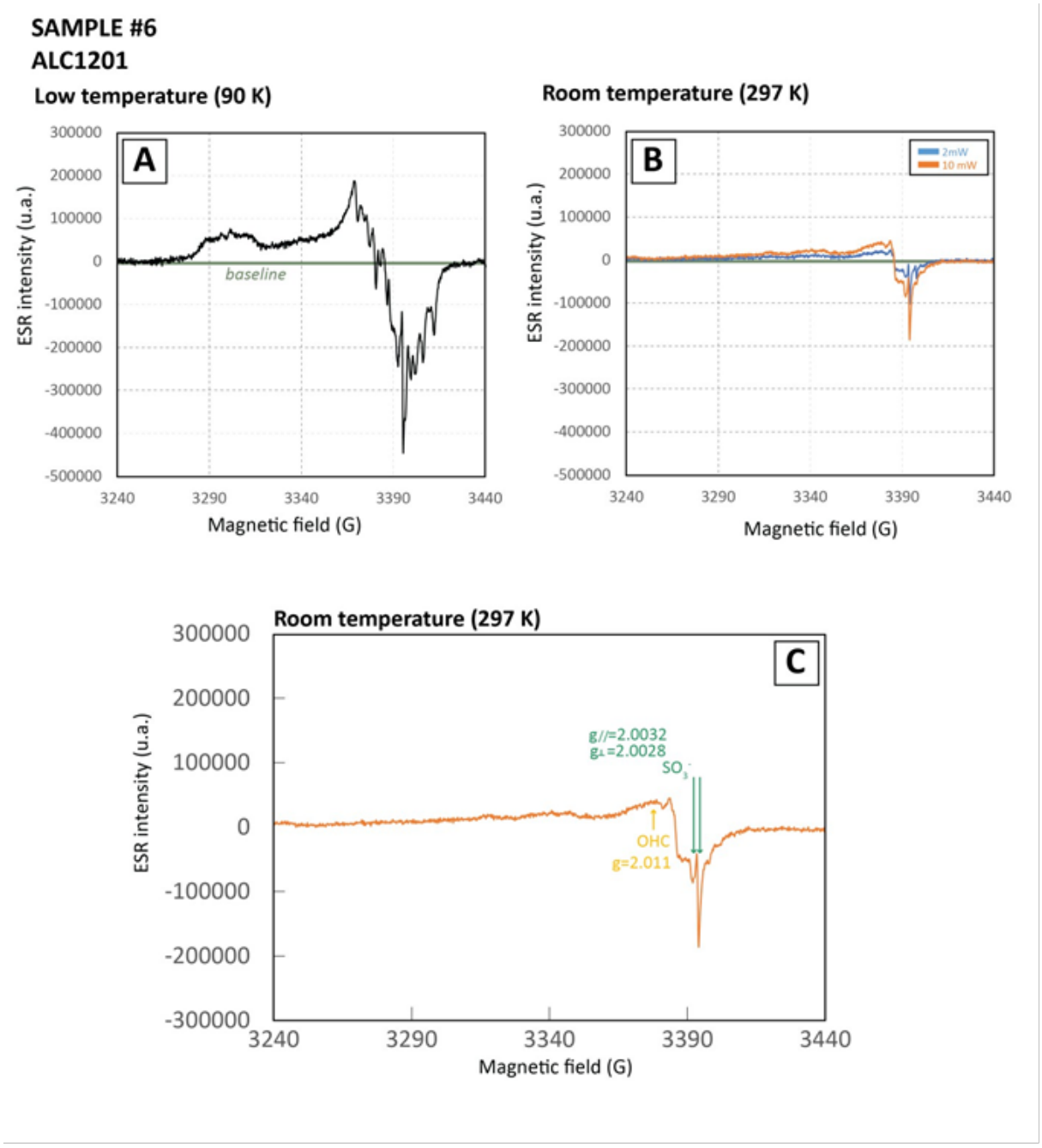

Figure S17. Comparison of the natural spectra of the sample #7 at low temperature (A), at room temperature with 2 mW and 10 mW (B). A basic visualization of the signal at room temperature is given in C.

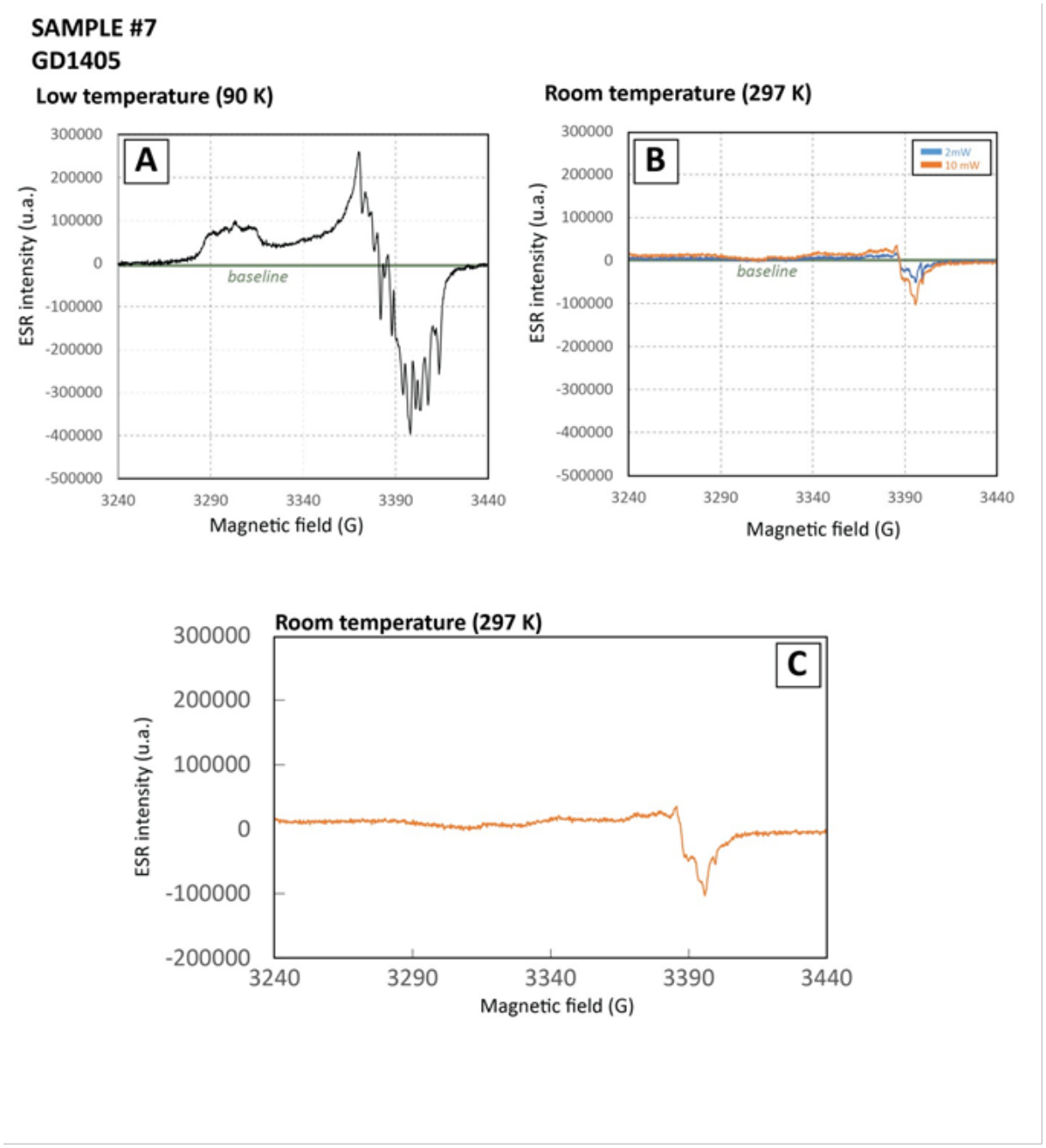

Figure S18. Comparison of the natural spectra of the sample #8 at low temperature (A), at room temperature with 2 mW and 10 mW (B). A basic visualization of the signal at room temperature is given in C.

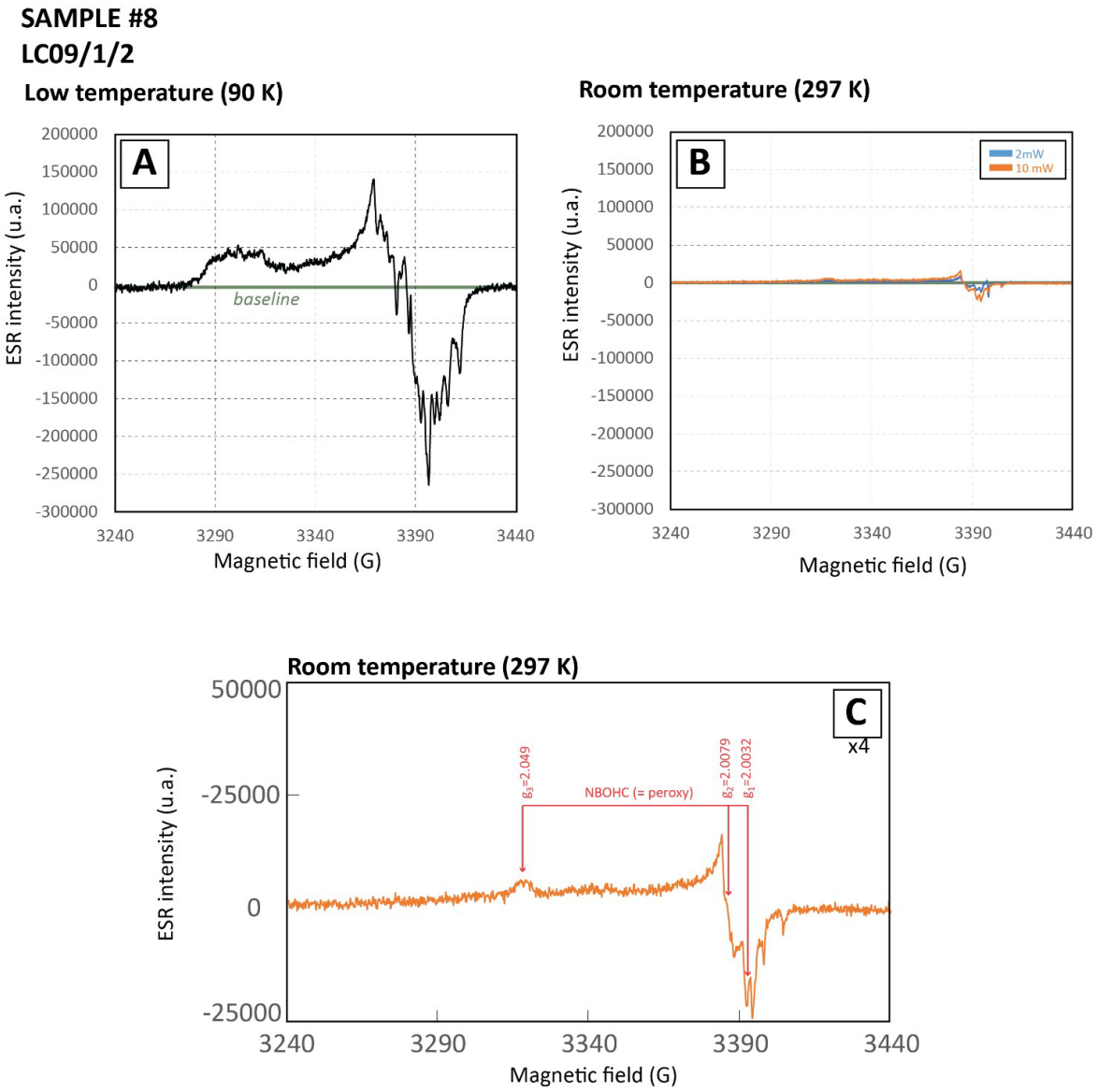

Table S1. Number of positive (+) and negative (-) peaks identified for various quartz samples, including the eight of the present study (*). For sample #4, the spectrum is very noisy, inducing a possible bias on the peaks counting.

Sample	Context	Peaks +	Peaks -	Total	Fraction (µm)	References
Terra Amata	Aeolian (dune)	12	12	24	40-160	Yokoyama et al. (1985)
Pure quartz	Artificial	12	12	24	30-50	Lin et al. (2006)
ROX 1.14	Aeolian (loess)	11	11	22	125-180	Kabacińska and Timar-Gabor (2022)
STY 1.10	Aeolian (loess)	10	10	20	125-180	Kabacińska and Timar-Gabor (2022)
2 MV 80	Aeolian (loess)	8	8	16	63-90	Kabacińska and Timar-Gabor (2022)
OUC1102-300 (#1)*	Fluvial	14	14	28	100-200	This study
KT04-2-2 (#2)*	Aeolian (dune)	16	16	32	180-250	Ben Arous et al. (2022)
SF05-2-4 (#3)*	Aeolian (dune)	12	12	24	180-250	Ben Arous et al. (2022)
CAC1203 (#4)*	Fluvial	12	12	24	100-200	García-Vadillo et al (2021)
CUB1004 (#5)*	Fluvial	14	14	28	100-200	Duval et al. (2017)
ALC1201 (#6)*	Fluvial	14	14	28	100-200	Duval et al. (2015)
GD1405 (#7)*	Fluvial (karst)	13	13	26	100-200	Duval et al. (2022)
LC09-1-2 (#8)*	Aeolian (dune)	14	14	28	180-250	Ben Arous et al. (2022)

References

Ikeda, S., Neil, D., Motoji, I., Kai, A., Miki, T., 1992. Spatial variation of co2 and so3 radicals in massive coral as environmental indicator. Jpn. J. Appl. Phys. 31, L1644–L1646. https://doi.org/10.1143/JJAP.31.L1644

Ryabov, I.D., Bershov, L. V., Speranskiy, A. V., Ganeev, I.G., 1983. Electron paramagnetic resonance of PO32- and SO3- radicals in anhydrite, celestite and barite: the hyperfine structure and dynamics. Phys. Chem. Miner. 10, 21–26. https://doi.org/10.1007/BF01204322